Eksplorium
Volume 43 No. 2, November 2022: 59–70

p-ISSN 0854-1418
e-ISSN 2503-426X

Volcanic Ash Fall Hazard of Mount Merapi on Yogyakarta Nuclear Area

Abimanyu Bondan Wicaksono Setiaji[1,3]*, Iman Satyarno[1], Agung Harijoko[2]
[1]Departement of Civil and Environmental Engineering, Universitas Gadjah Mada,
[2]Departement of Geological Engineering, Universitas Gadjah Mada
Grafika Bulaksumur St., No. 2, Yogyakarta, 55284, Indonesia
[3]Bureau for Organization and Human Resources, National Research and Innovation Agency (BRIN)
B.J. Habibie Building, Thamrin St., No. 8, Jakarta, 10340, Indonesia
*E-mail: abimanyubondan@mail.ugm.ac.id

Article received: 4 October 2022, revised: 12 November 2022, accepted: 30 November 2022
DOI: 10.17146/eksplorium.2022.43.2.6708

ABSTRACT

The existence of nuclear installations in the Yogyakarta Nuclear Area is vulnerable to the eruption of Mount Merapi, the most active volcano in Indonesia. Tephra hazard has the potential to threaten the operational activities of nuclear installations in the Yogyakarta Nuclear Area; thus, it is necessary to analyze the distribution and potential hazard of volcanic ash from Mount Merapi for future eruptions. Numerical modelling is used in analyzing tephra distribution using TEPHRA2 software with parameters of the 2010 Mount Merapi eruption, which is then visualized to isomass and isopach maps of tephra distribution. The analysis resulted in the ash dispersion leading to the Yogyakarta Nuclear Area in April, May, June, and August with an accumulated mass of 20-50 kg/m^3 with a thickness of 0.2-12 cm. It is necessary to deal with volcanic ash hazards such as roof strength, secondary cooling system, filtering system, and electrical system for several installations in the Yogyakarta Nuclear Area.

Keywords: Merapi, tephra hazard, nuclear area.

INTRODUCTION

The Yogyakarta Nuclear Area is a research center area in Yogyakarta. This area includes several facilities, some of which conduct research using radioactive materials. Nuclear installations in this area are designed, built, and operated following the safety and security requirements set by national and international regulations and safety standards [1]–[3]. Several work units located in the Yogyakarta Nuclear Area can be seen in Table 1. Mount Merapi is one of the most active volcanoes in Indonesia and is located 30 km north of the Yogyakarta Nuclear Area. The main threat from Mount Merapi is a Pyroclastic Density Current (PDC) or commonly referred to as "Wedus Gembel" in local terms, lava flows, lahars, and rock ballistic projectiles [4].

Table 1. Nuclear facilities and support infrastructures location within the Yogyakarta Nuclear Area.

No	Name of Installation
1	Kartini Research Reactor
2	Neutron Activation Laboratory
3	Radioactive waste Treatment
4	Environmental Laboratory
5	Indonesian Nuclear Technology Polytechnic
6	Nuclear Fuel Fabrication
7	Particle Physics (Electron Beam Machine (MBE) facility)
8	Laboratory of Material Processing Research

Figure 1 shows the disaster-prone areas of Mount Merapi. The site is divided into three (3) zones, namely disaster-prone areas I, II, and III, which are divided based on the potential hazard of the eruption product Mount Merapi.

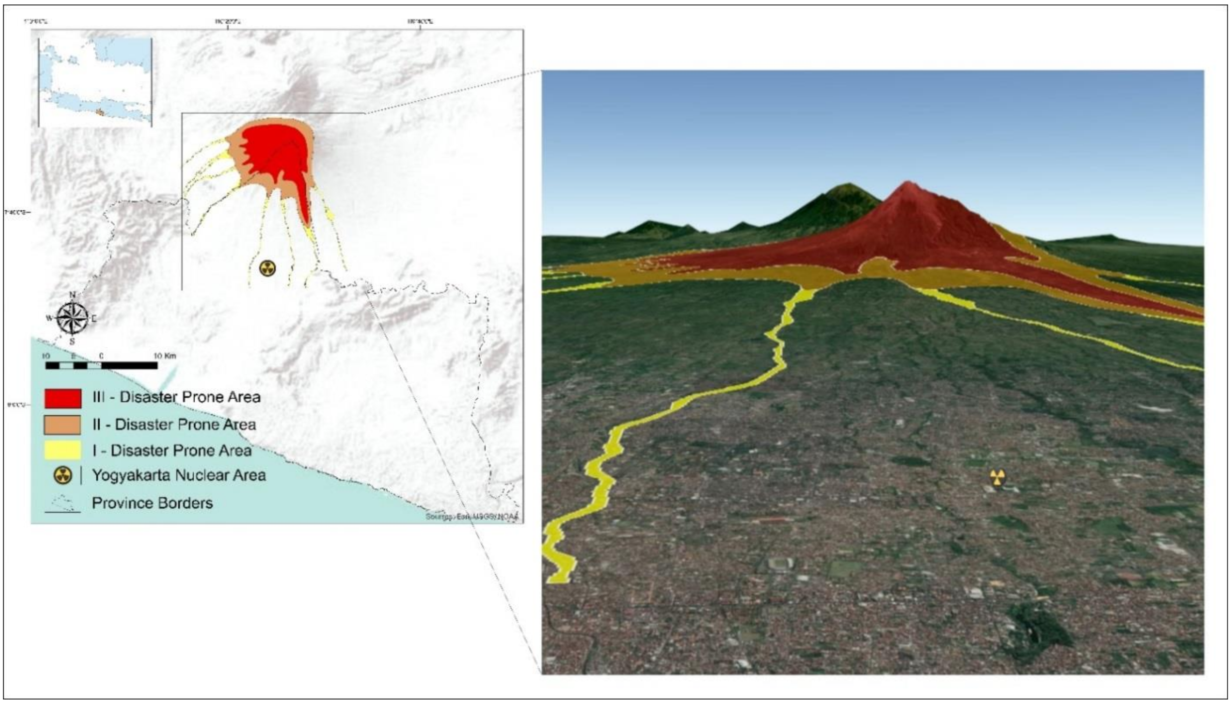

Figure 1. Location of the Yogyakarta Nuclear Area to the Disaster-Prone Area of Mount Merapi [4].

Based on the location of the Yogyakarta Nuclear Area, which is located outside the Disaster-Prone Area of Mount Merapi, to avoid the primary dangers of the eruption of Mount Merapi, such as pyroclastic density current, stone ballistic projectiles and lava flows, however, a large eruption that occurred in 2010 caused secondary hazards of eruption products, specifically volcanic ash (tephra) from the eruption to the Yogyakarta Nuclear Area which has the potential to disrupt the operations of this research area. Hence, it is necessary to research the dangers of volcanic ash fall to research facilities in this area of interest to anticipate major eruptions from Mount Merapi in the future that will impact the Yogyakarta Nuclear Area.

THEORY

Volcanic Ash Distribution

The surface wind's profiles are usually different in direction and speed than winds higher in the atmosphere. The height of the eruption column significantly affects the dispersion of volcanic ash. In addition to the wind factor, distribution is also influenced by the size, shape, and density of ash particles and the magnitude of the eruption. The larger and heavier fragments usually fall closer to the eruption source, while the lighter fragments are scattered further upwind [5].

Hazards of Volcanic Ash on Infrastructure

Specific factors that must be considered in the tephra hazard assessment of a nuclear reactor facility include:

- **Bearing strength of building structures**: The loading of structures by volcanic ash increases directly with the thickness and density of the ash. Dry ash consists of glass and pumice and has an average density of about 500 kg/m^3. An example of the eruption of Mount St. Helens, which falls when it rains or gets wet shortly after falling, has an average density of 1030-1250 kg/m^3 [6]. Dome-shaped roof buildings can reduce the potential for ash build-

p-ISSN 0854-1418
e-ISSN 2503-426X

up on the roof so that the danger of loading on the roof can be avoided [7]. Table 2 shows the strength of several types of construction and roof classes to the static loads caused by the accumulation of volcanic ash. In contrast, Table 3 shows the slope angle of several roofing materials to allow volcanic ash accumulation on the roof surface.

Table 2. Types of roof construction to the volcanic ash loads [8].

Construction Types	Roof Class	Roof Class Description	Mean – Range Collapse Load (kg/m^2)
Light wood frame Weak masonry	A	Weak timber board on timber rafters/trusses Metal sheet roof on timber rafters/trusses in poor condition Tiles on timber rafters/trusses in poor condition Vaulted masonry	184 (122 - 265)
Light Metal	B	Long-span roofs with metal sheets or fibre-reinforced concrete sheets	204 (143 – 296)
Unreinforced Masonry Reinforced concrete with wood of metal roof deck	C	Metal sheet roofs on timber rafters/trusses in average condition Tiles on timber rafters/trusses in average condition	296 (194 – 418)
Heavy Timber Structural masonry Steel frame with wood or metal roof deck	D	Metal sheet roofs on timber rafters/trusses in good condition Strong timber on timber rafters/trusses in good condition	408 (275 – 601)
Reinforced concrete with concrete roof deck Precast with concrete roof deck Steel frame with concrete roof deck	E	Flat reinforced concrete roof designed for access and generally in good condition	714 (489 – 1050)

Table 3 Maximum slope angle of some roofing materials to drain volcanic ash from the roof surface [9].

Roof Material	Minimum slope angle (^{o})		
	Dry	Moist	Wet
Tile	38	40	50
Asbestos	37	39	41
Metal Sheet	37	38	40

- **Filtration system**: Water and air filtration systems can become clogged by ash ingress into the water supply and air filtration systems. Fine particles of volcanic ash size in micrometres adhere to the surface of the filter system, which can disrupt the performance of the water and air filter systems [6].
- **Machinery**: Moving engine parts can be eroded by abrasive ash particles, resulting in wear or damage. Machine components located outside the building, uncovered, or potentially exposed to volcanic ash are extremely vulnerable to losing function prior to cleaning [10]. The abrasive and corrosive nature of volcanic ash causes engines exposed to it to perform poorly and wear out quickly.
- **Electrical system**: Volcanic ash can cause electrical disturbances in the form of short circuits in electrical

components covered with fine ash (Flashover). Flashover can occur when dry insulator strings are uniformly coated with fine-grained volcanic ash. Fine grain ash is non-conducting and does not cause a large enough leakage current over the insulator surface; when water vapour collects on the insulator surface, the fine ash material will form a conductor, resulting in a leakage current. Electrical conductivity in wet conditions, volcanic ash is very high, so it can cause sparks and short circuits when covering conductors in power lines [11]. Volcanic ash can corrode electrical equipment if the cleaning process is not carried out immediately [12].

- **Water cooling system**: An exposed cooling pool can be affected in two ways: low-density volcanic ash and finer ash grains that float on the surface and will create a fairly thick layer during volcanic ash exposure. The denser ash material will sink, settle, and reduce reservoir capacity, clog filters, and reduce or completely stop circulation [13].
- **Indirect effects**: The 1980 eruption of Mt St Helens, building structures, vehicles, other machinery, and roads can be adversely affected over a large area. This effect can persist because maintenance systems and emergency services are disrupted and because of the eruption's impact. The maintenance personnel responsible for the operation and safety of the reactor were unable to perform their duties properly due to difficulty breathing and limited vision. Emergency staff and personnel could not access the reactor because vehicles were damaged or roads were covered with thick volcanic ash during the eruption. Many vehicles, including emergency vehicles, could not move because the air filter was clogged with ash. In addition, the ash also clogs the fuel injection system for several types of vehicles. Reactor personnel may refuse to leave their families and homes in an emergency [14].

TEPHRA2

Volcanic ash distribution simulation was performed using TEPHRA2 software. TEPHRA2 is a software with a numerical model for simulating tephra fall from explosive volcanic eruptions designed to predict the dispersion of volcanic ash and small rock fragments that erupt into the atmosphere during volcanic eruptions. TEPHRA2 is implemented open source on VHub.org and designed for disaster research in assuming and forecasting the hazard of tephra dispersion. The vertical volcanic ash column (Plume) height is above the vent, where the particles are carried by the wind and scattered from the top of the *plume* towards the wind blowing at that time. The plume height is divided into sections where the particles fall and spread from each section. The equation used is equation no (1) as follows:

$$M(x,y) = \sum_{i=1}^{H} \sum_{j=\Phi_{min}}^{\Phi_{max}} M_{i,j}^{0} f_{i,j}(x,y) \qquad (1)$$

Where $M_{i,j}^{0}$ is the initial mass in column /plume i for particles of grain size j, function $f_{i,j}(x,y)$ is the formula for calculating the mass fraction for certain particles and heights that fall at a specific point coordinates (x,y). H is the maximum puff height, and j is the grain size of the pyroclastic material. A network of

p-ISSN 0854-1418
e-ISSN 2503-426X

grid receptors is made around the volcano, including the coordinate parameters (Easting and Northing) and the elevation of the receiving point [15]. This software uses the Advection-Diffusion equation [16], then combines the calculations with the following equation:

$$f_{i,j}(x,y) = \frac{1}{2\pi\sigma_{i,j}^2} exp\left\{-\frac{\left(x-\bar{x}_{i,j}\right)^2 + \left(y-\bar{y}_{i,j}\right)^2}{2\sigma_{i,j}^2}\right\} \quad (2)$$

Where the function $f_{i,j}(x,y)$ is the solution according to the Advection-Diffusion Equation to calculate the mass for a certain particle size and a certain release height that falls around the coordinate point(x,y). Parameter $\bar{x}_{i,j}$ and $\bar{y}_{i,j}$ are the coordinates of the center point of the Gaussian distribution ($\bar{x}_{i,j} = x_i + \sum_{lapisan} \delta\, x_j$, $\bar{y}_{i,j} = y_i + \sum_{lapisan} \delta\, y_j$) and $\sigma_{i,j}^2$ are the variance of the Gaussian distribution which is a function of atmospheric diffusion and the horizontal distribution of volcanic ash emissions [17]. With this equation, the TEPHRA2 program can mathematically describe the movement and dispersion of volcanic ash as it leaves the eruption column, falls on the atmosphere layer, and reaches the mainland. The output model is the mass of volcanic ash accumulation with units of kg/m^2.

METHODOLOGY

Research parameter data were obtained, as shown in Table 4. The analysis method for the distribution of volcanic ash was carried out using the TEPHRA2 software. The modelling results are used to analyze the vulnerability of the research area of tephra hazards. The TEPHRA2 software uses three (3) main parameters: determining a receptor grid, meteorological data, and eruption parameters.

Table 4. Research data.

Data	Description
Administrative boundaries	The boundary of the research area
DEM (Digital Elevation Model)	Grid receptors analysis
Wind speed and wind direction	Input simulation parameters
Eruption parameter	Input simulation parameters

Volcanic Ash Receptor

The receptor grid or volcanic ash receiver network aims to capture volcanic ash that falls to the ground as a result of the simulation. The simulation is run on a grid measuring 100 km × 100 km with a distance between grid points of 3 km on the x and y axes, containing the coordinates (X and Y) and elevation at each grid point. The shape and dimensions of the receptor grid are made in a square shape with Mount Merapi in the middle and covers the entire of Yogyakarta Special Region. This grid model aims to capture the distribution of volcanic ash in all directions according to wind direction, and information for tephra distribution to Yogyakarta Province was obtained. The number of grid points can be expanded to determine the spatial pattern of volcanic ash distribution over a larger area, taking into account the longer simulation time. The distribution of the grid is in Figure 2.

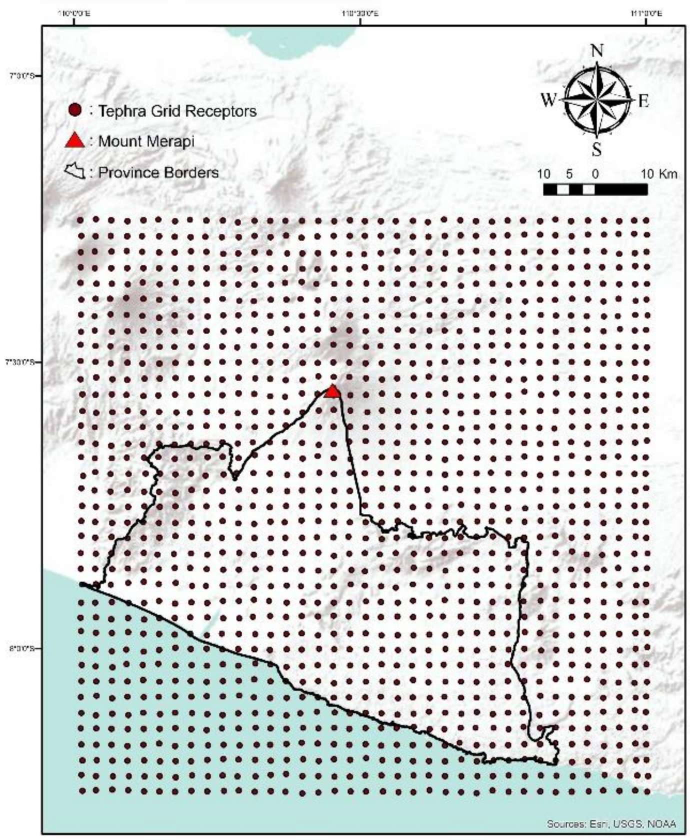

Figure 2. The distribution of the receptor grid for the tephra fall of Mount Merapi.

Meteorology

Meteorological conditions around the volcano influence the dispersion of tephra during an eruption. The data taken are wind speed data and wind directions. Meteorological data used is data from meteorological observations for about five years (2017-2021) from the Pasarbubar weather station, which is operated by Research and Technology Development for Geological Mitigation (BPPTKG) Yogyakarta and located about 300 m southwest of the peak of Mount Merapi as surface data, with an altitude of 2676 masl. Wind direction data above the Pasarbubar weather monitoring sensor are obtained from wind data/reanalysis of the National Centers for Atmospheric Prediction (NCEP), and the National Center for Atmospheric Research (NCAR) downloaded on the National Oceanic and Atmospheric Administration (NOAA) website. Data availability provided from an altitude of 5 km, 15 km, and 25 km due to the peak height of the plume column of the Merapi eruption in 2010 is 17 km [18], and the data taken is data at an altitude of 5 km and 15 km. The monthly wind profile used as input for eruption parameters and the height of the weather sensor at the observation station became a reference point which is then included in Equation 3 to change the wind speed data to various altitude points as vertical extrapolation to the maximum plume.

$$v_1 = v_2 \left(\frac{z_1}{z_2}\right)^p \qquad (3)$$

The v_1 and v_2 are the wind speed at heights 1 and 2 in m/s, the z_1 and z_2 are altitudes at height 1 and altitude at height 2 in meters, while p is a function of atmospheric stability [19].

p-ISSN 0854-1418
e-ISSN 2503-426X

Eruption Parameter

Input parameters for the eruption of Mount Merapi were primarily obtained from the Research and Technology Development For Geological Mitigation (BPPTKG) Yogyakarta database for the 2010 eruption of Mount Merapi and from other data literature which discusses the 2010 Merapi eruption. Eruption parameters can be seen in the following table:

Table 4. Input parameters for the 2010 Merapi eruption [20]–[22].

Input Parameter	Value
Total plume height (m)	17000
Eruption mass (kg)	3.1e+11
Maximum grain size (phi)	1
Minimum grain size (phi)	4
Median grain size	2.5
Standard deviation	1.5
Vent easting	438902
Vent northing	9166368
Vent elevation (m)	2839
Eddy Constant	0.04
Diffusion coefficient	568
Fall time threshold (second)	100.000
Lithic density (kg/m^3)	2.600
Pumice density (kg/m^3)	1.000

TEPHRA2 software simulation produces numerical data output of tephra weight received by each receptor point. This data is then spatially interpolated using the Kriging method on ArcGIS software. The receptor points that already have a value for the weight of tephra from the simulation output, isomass maps, and isopach maps can be constructed to show the ash load value and spatial thickness.

RESULTS AND DISCUSSION

Tephra Dispersion Model

According to the simulation results, each month's trend in volcanic ash dispersion is distinct. Gunung Kidul Regency, Klaten Regency, Surakarta City, and some parts of Boyolali Regency and Sleman Regency, which are close to Mount Merapi's peak, are among the regions exposed to volcanic ash from January through March due to the pattern of tephra distribution, which points in an east-southeast direction. Volcanic ash tends to be distributed southwest throughout June, July, and August. Kulon Progo Regency, Purworejo Regency, and some parts of Magelang Regency and Sleman Regency, which is the area on the west side of Mount Merapi, will be exposed to volcanic ash in the June and July segments, while the southern region of Mount Merapi is more susceptible to volcanic ash in August. The most severe exposure will be in Sleman Regency, and gradually Gunung Kidul, Yogyakarta, Bantul, and Kulon Progo Regencies will probably be exposed to the volcanic ash, which will be thinning toward the south direction. Volcanic ash tends to be distributed west to the north from September to December. Volcanic ash will primarily affect the west regions of Merapi Peak, including Kulon Progo Regency, Purworejo Regency, and portions of Magelang and Sleman Regencies. The distribution of volcanic ash that directly leads to and affects the Yogyakarta Nuclear Area occurs in April, May, June, and August. The total mass of accumulated tephra is presented as Isomass map, which shows the mass per unit area. The thickness of the accumulated volcanic ash is depicted by an isopach map in centimetres (cm). Figure 3 shows isomass and isopach maps of volcanic ash distribution for each month.

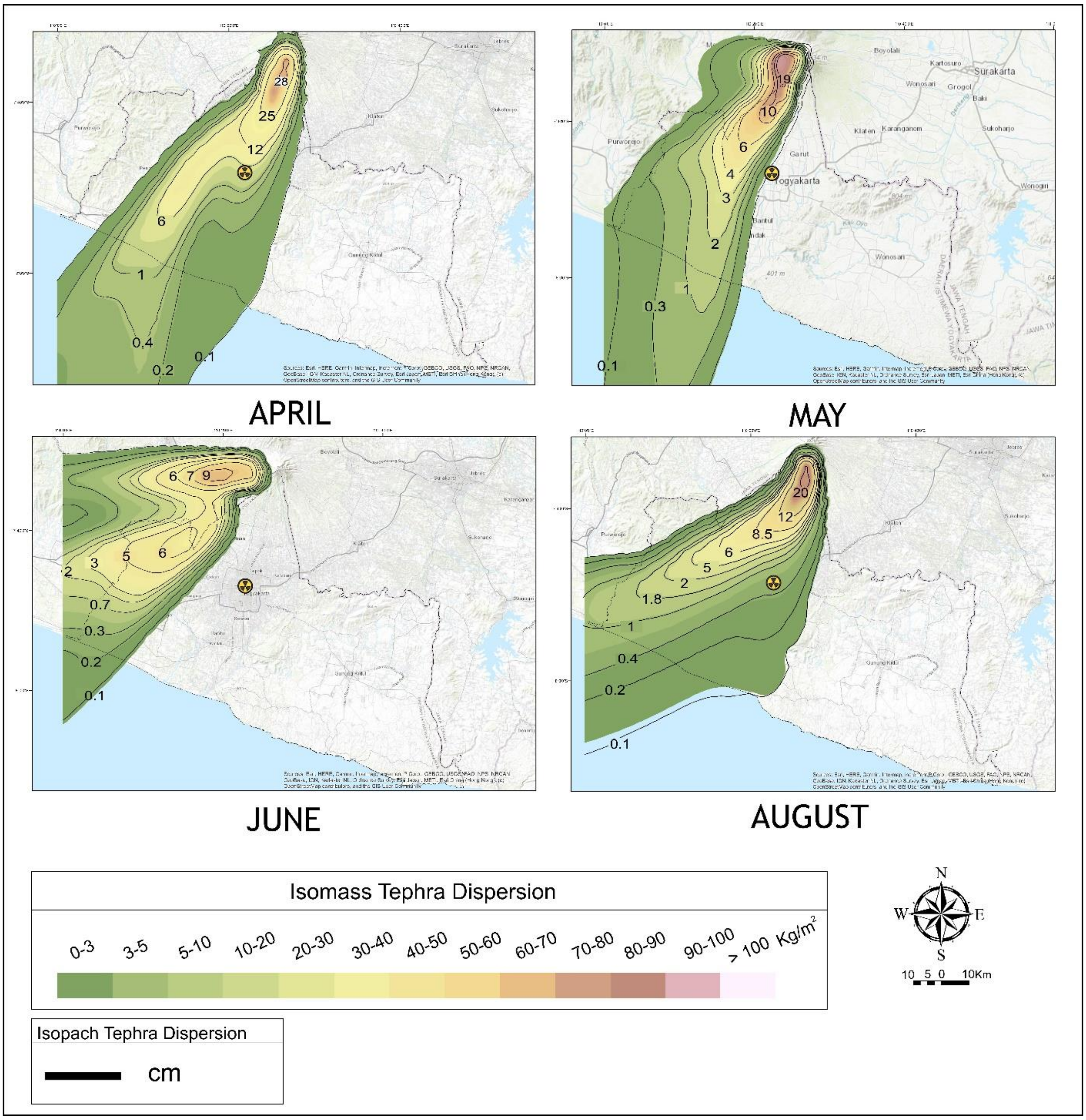

Figure 3. Isomass and isopach map of volcanic ash distribution to the Yogyakarta Nuclear Area.

Tephra Hazard to the Yogyakarta Nuclear Area

The area with the most significant threat in Yogyakarta Nuclear Area is the Kartini Reactor facility which stores nuclear fuel in the reactor core. The Kartini Research Reactor has several safety systems intended to ensure high safety of reactor operation. The safety system operates using the "*fail safe*" principle, which means that the Kartini Research Reactor remains safe in the event of a system failure. Whenever an operational event occurs, it can be anticipated either internally or externally, and the reactor will experience an automatic blackout (scram or shutdown) [23]. The risk of a nuclear accident can come from the malfunction of the Kartini Reactor operating system, resulting in an operating accident condition outside the design basis of the Reactor or Beyond Design Basis Accident (BDBA). The Kartini Reactor is used for research, irradiation, education, and training. The Yogyakarta Nuclear Area is close to educational institutions, residential areas, shops, hotels, and shopping malls.

The most dangerous nuclear hazard is caused by a malfunction of the Kartini Reactor operating system, which can occur if the containment building collapses. The incident caused radioactive leaks and radiological effects in the environment that were dangerous to the public. The most radioactive substances released into the environment due to reactor operations are Iodine 131 (I_{131}) and the noble gasses Krypton and Xenon (Kr, Xe). However, other gaseous fission products are also released [24]. This condition is possible if the infrastructure of the Kartini Reactor building is damaged or collapses into the reactor core. Figure 4.A illustrates the reactor building. Radioactive substances released into the environment impact water, soil, and air. The magnitude of radioactive substance release and displacement behaviour will determine the intensity of the impact. Iodine 131 (I_{131}) is a radioactive substance that can be released into the environment of concern and has a deterministic effect or impacts that occur directly and stochastic effects or long-term impacts on the society that arise when exposed to substances through open wounds or inhalation process.

The potential danger of volcanic ash to the reactor is the static loading of volcanic ash on the roof of the containment building, which causes the building to collapse. The containment building of the Kartini reactor is made of dome-shaped concrete. The mass of volcanic ash, according to Table 2, is 754 kg/m^3 or greater, which has the potential of failure due to roof collapse. Ash that falls on the roof may collect in the reactor's gutter system, potentially causing blockages and partial load in the gutter system. According to the modelling results, the volcanic ash that reached the Yogyakarta Nuclear Area ranged from 20 to 50 kg/m^3. The cooling system in the Kartini Reactor is divided into two parts: the primary cooling system and the secondary cooling system. Heat exchangers and demineralized cooling water are used in the primary cooling system. If the water in the reactor core reaches 45^{o}C, the reactor is shut down, and the cooling process begins. A pump is used to push cool water through the tank. A cooling tower is used for the secondary cooling system, as shown in Figure 4.A. The primary and secondary systems dissipate heat generated by the fission reaction during reactor operation [25]. Volcanic ash can affect the reactor cooling process. The cooling water in the primary cooling system is stored in an enclosed tank to avoid being affected by volcanic ash exposure. Volcanic ash, on the other hand, can cover the air filter system in the reactor cooling tower, which is part of the secondary cooling system. As a result, the cooling process in the secondary cooling system may be affected prior to the ash-cleaning process. Volcanic ash falling into the pond in front of the Kartini Reactor, as depicted in Figure 4.B, will also impact installations that use pool water. This pool was previously used as a primary cooling water reservoir. Still, it is no longer used when the primary cooling water is stored in a tank in an enclosed space, but it is still used in several Yogyakarta Nuclear Area facilities. Volcanic ash can impact the performance of facilities that use pool water. The Electron Beam Machine (MBE) facility in the Yogyakarta Nuclear Area is shielded from volcanic ash inside the building, so these facilities are not affected by tephra hazards.

Volcanic ash may also have an impact on the Indonesian Nuclear Technology Polytechnic, which is located in the Yogyakarta Nuclear Area. This facility is not a nuclear facility but rather a learning facility for the utilization of nuclear energy, so the tephra hazard to this facility needs to be assessed. Respiratory and visual disturbances disrupt this facility during teaching and learning activities in the Polytechnic environment. The Polytechnic's building structure is made of concrete and tile materials, and the slope factor significantly impacts the roof structure's durability, as shown in Table 3. The slope roof significantly impacts the accumulation of ash over it; the greater the slope of the roof, the better the roof is at passing the accumulated ash. Table 3 shows the potential for volcanic ash with dry, moist, and wet conditions on the roof's slope for various materials. Figure 4.C shows polytechnic buildings with numerous ventilation openings. Volcanic ash is prone to entering buildings and adhering to installations susceptible to volcanic ash's abrasive and corrosive properties.

Figure 4. Infrastructure buildings in the Yogyakarta Nuclear Area.

CONCLUSION

The analysis results for the dispersion of volcanic ash show that the distribution of volcanic ash that leads to the Yogyakarta Nuclear Area is on April, May, June, and August, affecting several installations. Electrical systems that are not covered have the potential for flashovers. The containment building of the Kartini Research Reactor is in a dome-shaped building so that it can pass volcanic ash on the roof of the reactor building. Still, the ash will accumulate in the gutter system and can cause blockages during the rainy season. The secondary cooling system of the Kartini Research Reactor that uses a cooling tower has the potential to be disrupted due to volcanic ash covering the top of the tower. Buildings that use a roof system in the form of tiles and metal sheet roofs on timber rafters/trusses have the potential to damage or collapse due to static loads from the accumulation of volcanic ash.

p-ISSN 0854-1418
e-ISSN 2503-426X

ACKNOWLEDGMENT

The authors would like to appreciate National Research and Innovation Agency (BRIN) for financial research through the SAINTEK scholarship, and the authors also thank Dr. Agus Budi Santoso as Head of Research and Technology Development For Geological Mitigation (BPPTKG) for the support of data and input during this research, and for all parties who have given suggestions and directions for the final manuscript.

REFERENCES

[1] BAPETEN, *Perka BAPETEN tentang Keselamatan Operasi Reaktor Non Daya*. Indonesia, 2019.
[2] BAPETEN, *Perka BAPETEN tentang Evaluasi Tapak instalasi Nuklir Aspek Kegunungapian*. Jakarta: jdih.bapeten.go.id, 2015.
[3] IAEA, *SSR-3 Safety of Research Reactors*, no. May. Viena, Austria, 2016.
[4] D. S. Sayudi, N. A, D. Djalal, and M. Muzani, “Peta Kawasan Rawan Bencana Gunung Merapi,” Bandung, 2010.
[5] C. Bonadonna and A. Costa, “Estimating the volume of tephra deposits: A new simple strategy,” *Geology*, vol. 40, no. 5, pp. 415–418, 2012.
[6] A. M. Sarna-Wojcicki, S. Shipley, R. B. Waitt, D. Dzurisin, and S. H. Wood, “Areal distribution, thickness, mass, volume and grain size of air- fall ash from the six major eruptions (of Mount St. Helens) of 1980.,” *U.S. Geol. Surv. Prof. Pap.*, vol. 1250, pp. 577–600, 1981.
[7] I. Satyarno, “Rumah Dome sebagai Bangunan Alternatif pada Daerah Rawan Bencana Gunung Berapi,” in *Simposium Gunung Merapi: Kajian Perilaku, Dampak dan Mitigasi Bencana Akibat Erupsi Merapi 2010*, 2011.
[8] R. J. Blong *et al.*, “Estimating building vulnerability to volcanic ash fall for insurance and other purposes,” *J. Appl. Volcanol.*, pp. 1–13, 2017.
[9] F. Akbar, “Model Atap Rumah yang Tanggap terhadap Abu Pasir Vulkanik,” Universitas Brawijaya, 2014.
[10] S. F. Jenkins, R. J. S. Spence, J. F. B. D. Fonseca, R. U. Solidum, and T. M. Wilson, “Volcanic risk assessment : Quantifying physical vulnerability in the built environment,” *J. Volcanol. Geotherm. Res.*, vol. 276, pp. 105–120, 2014.
[11] J. B. Wardman, T. Wilson, J. Cole, P. S. Bodger, and D. M. Jhonston, “Quantifying the Vulnerability of High Voltage Power Transmission Systems to Volcanic Ashfall Hazards,” in *EEA Conference & Exhibition 2010 , Christchurch*, 2010.
[12] T. Wilson, M. Daly, and D. Johnston, “Review of Impacts of Volcanic Ash on Electricity Distribution Systems, Broadcasting and Communication Networks,” Auckland, 2009.
[13] T. M. Wilson *et al.*, “Volcanic ash impacts on critical infrastructure,” *Phys. Chem. Earth*, vol. 45–46, pp. 5–23, 2011.
[14] S. Shipley and A. M. Sarna-Wojcicki, “Distribution, Thickness, and Mass of Late Pleistocene and Holocene Tephra From Major Volcanoes In The Northwestern United States: A Preliminary Assesment of Hazard From Volcanic Ejacta to Nuclear Reactors In The Pacific Northwest,” 1980.
[15] L. Courtland, C. Connor, L. Connor, and C. Bonadonna, “Introducing Geoscience Students to Numerical Modeling of Volcanic Hazards: The example of Tephra2 on VHub.org,” *Numeracy*, vol. 6, no. 2, 2012.
[16] T. Suzuki, “A Theoretical Model for Dispersion of Tephra,” *Arc Volcanism; Phys. Tectonics*, pp. 95–113, 1983.
[17] Bonadonna, “Plume height, volume, and classification of explosive volcanic eruptions based on the Weibull function,” *Bull. Volcanol.*, vol. 75, no. 8, pp. 1–19, 2013.
[18] J. S. Pallister *et al.*, “Merapi 2010 eruption-Chronology and extrusion rates monitored with satellite radar and used in eruption forecasting,” *J. Volcanol. Geotherm. Res.*, vol. 261, pp. 144–152, 2013.
[19] J. F. Newman and P. M. Klein, “The Impacts of Atmospheric Stability on the Accuracy of Wind Speed Extrapolation Methods,” *Resources*, vol. 3, pp. 81–105, 2014.
[20] Sunarko, “Jurnal Pengembangan Energi Nuklir Kajian Probabilistik Jatuhan Abu Vulkanik Terhadap Tapak Pembangkit Listrik Tenaga Nuklir (PLTN) Muria,” *J. Pengemb. Energi Nukl.*, vol. 18, no. 1, pp. 49–57, 2016.
[21] L. D. Setiadji, J. Jane, N. G. Situmorang, and A. Wiguna, “Erupsi merapi 2018: interpretasi jenis erupsi berdasarkan studi material vulkanik hasil erupsi eksplosif 11 mei dan 1 juni 2018,” in *Seminar Nasional Kebumian Ke-11*, 2018, no. September, pp. 908–917.
[22] Surono *et al.*, “The 2010 explosive eruption of Java’s Merapi volcano-A ‘100-year’ event,” *J. Volcanol. Geotherm. Res.*, vol. 241–242, pp. 121–135, 2012.
[23] BAPETEN, “Laporan Keselamatan Nuklir 2009,” Jakarta, 2010.
[24] PSTA BATAN, “Rencana Kontinjensi Reaktor Kartini,” Yogyakarta, 2016.

[25] PSTA BATAN, "Laporan Analisis Keselamatan Reaktor Kartini," Yogyakarta, 2019.